States in ^{196}Pt observed with the $(n,n'\gamma)$ reaction

E. Tavukcu,[1,*] L. A. Bernstein,[2] K. Hauschild,[2,†] J. A. Becker,[2] P. E. Garrett,[2] C. A. McGrath,[2,‡] D. P. McNabb,[2] W. Younes,[2] P. Navrátil,[2] R. O. Nelson,[3] G. D. Johns,[3] G. E. Mitchell,[1] and J. A. Cizewski[4]

[1]*North Carolina State University, Raleigh, North Carolina 27695 and Triangle Universities Nuclear Laboratory, Durham, North Carolina 27708*

[2]*Lawrence Livermore National Laboratory, Livermore, California 94551*

[3]*Los Alamos National Laboratory, Los Alamos, New Mexico 87545*

[4]*Rutgers University, New Brunswick, New Jersey 08903*

(Received 24 December 2001; published 31 May 2002)

Levels in ^{196}Pt have been studied via the ^{196}Pt$(n,n'\gamma)$ reaction for a range of neutron energies from 1 to 8 MeV. A "white" spectrum of neutrons was produced at the LANSCE/WNR facility, and the incident neutron energy was determined by the time-of-flight technique. Analysis of measured $\gamma\gamma$ coincidence data and γ-ray excitation functions, obtained with the large-scale Compton-suppressed Ge spectrometer GEANIE, yielded 13 new levels and 24 new γ rays below $E_x=3$ MeV in ^{196}Pt. Interacting boson model (IBM) calculations with broken SO(6) dynamical symmetry were performed. A new experimental level was found to be a prime candidate for the $J^\pi=4^+$, $\sigma=6$, $\tau=5$ IBM state.

DOI: 10.1103/PhysRevC.65.064309 PACS number(s): 23.20.Lv, 21.10.−k

I. INTRODUCTION

The nuclei in the $A=180-200$ mass region exhibit a gradual shape change from prolate [1] to oblate [2] before the spherical limit is reached at $A=208$. As a result of the complex nature of these shape transitions, simple rotational and/or vibrational models do not adequately describe the nuclei in this region. The interacting boson model (IBM) [3,4] is very successful in interpreting the transition region consistently. In fact, ^{196}Pt has been shown to be a good example of the SO(6) limit of the IBM [5–7]. Many of the low-spin positive-parity states below the pairing energy gap in ^{196}Pt were identified and explained in terms of this model by Cizewski *et al.* [6]. In addition, platinum isotopes have been the focus of a variety of other experiments to search for mixed symmetry states [8], high-lying octupole states [9], octupole fragmentation [10], and scissors mode states [11–14]. Therefore, a number of experimental techniques have been applied to the study of ^{196}Pt, including Coulomb excitation [15–18], two-nucleon transfer [19,20], neutron capture (n,γ) [6,21], and neutron inelastic scattering $(n,n'\gamma)$ [22]. The result is a fairly detailed partial level scheme for ^{196}Pt for $E_x \leqslant 3$ MeV. However, as a result of the high density of states above 2 MeV in ^{196}Pt, many near-yrast states and their γ decays are as yet unknown.

The combination of a high-resolution Ge-detector array and a neutron spallation source allowed us to probe ^{196}Pt via a neutron-induced reaction and γ-ray spectroscopy. The neutron-induced reaction provides a method for the population of levels away from the yrast line at low excitation energies. The main advantage of the present study is that a low-energy γ ray originating from levels with energies greater than ≈ 1 MeV can be unambiguously placed using both $\gamma\gamma$ coincidences and excitation functions. A disadvantage is that spin assignments could not be made due to the low statistics in the individual detectors, preventing angular distribution measurements. A total of 13 new levels below $E_x=3$ MeV and their γ-ray branchings are reported here. DiPrete [22] also carried out ^{196}Pt$(n,n'\gamma)$ experiments that emphasized angular distribution measurements, but no $\gamma\gamma$ coincidence measurements were performed. The combination of these two data sets allowed spin and parity restriction on the new levels in ^{196}Pt.

II. EXPERIMENTAL DETAILS

The experiment was performed at the Los Alamos Neutron Science Center (LANSCE) Weapons Neutron Research (WNR) facility. Neutrons in the energy range from below 1 MeV to nearly 800 MeV are produced by spallation reactions of pulsed 800-MeV protons incident on a natural tungsten target. The proton beam consisted of 625-μs-long macropulses, each of which was subdivided into micropulses spaced 1.8 μs apart. These macropulses were produced at a frequency of 80 Hz, giving a 5% duty cycle. The energy of the reaction neutrons was determined by the time-of-flight (TOF) technique. The γ flash from the spallation reactions with the neutron production target was used as the reference time. The GEANIE (germanium array for neutron-induced excitations) spectrometer [23], located a distance of 20.34 m from the WNR spallation neutron source on a flight path at 60° to the right of the incident proton beam $(60R)$, was used for γ-ray spectroscopy. The neutron flux was deduced from a fission chamber counter [24] placed in the beam 1.86 m upstream from the GEANIE spectrometer.

A 9.94-g sample of 97.25% isotopically enriched ^{196}Pt, consisting of two 2.5-cm-diam disks with additional ^{196}Pt sandwiched in between, was placed at the focal point of the GEANIE spectrometer. The neutron beam spot on the ^{196}Pt

*Email address: tavukcu1@llnl.gov

†Present address: DAPNIA/SPhN CEA Saclay, Bat 703 l'Orme des Merisiers, F-91191 Gif-sur-Yvette, France.

‡Present address: Idaho National Engineering and Environmental Laboratory, P.O. Box 1625, Idaho Falls, ID 83415.

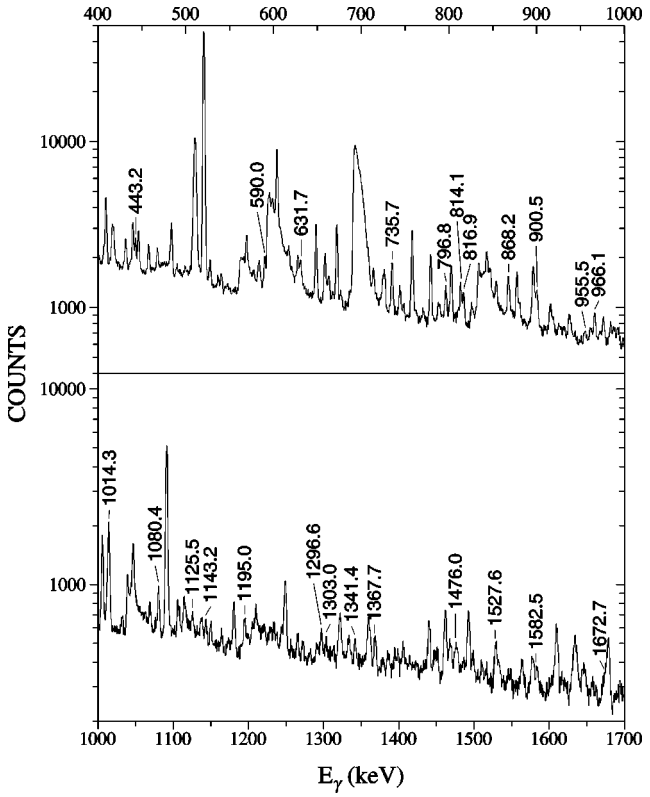

FIG. 1. The γ-ray spectra obtained from the sum of the coaxial Ge detectors for the ^{196}Pt$(n,n'\gamma)$ reaction in the $E_n=1-8$ MeV range. The new γ rays reported in this experiment are labeled with their energies in keV.

sample was 1.91 cm diameter. GEANIE included 11 planar and 15 coaxial Ge detectors [25% efficient relative to a 3 in.$\times$3 in. NaI(Tl) detector]. All planar and nine of the coaxial detectors were equipped with BGO escaped-suppression elements. In addition, all of the planar detectors were fitted with NaI nose-cone escaped-suppression elements. The planar detectors were grouped at the most forward and backward angles with respect to the beam direction, and γ-ray events with energies $E_\gamma \leqslant 1$ MeV were recorded for the planar detectors. The coaxial detectors were positioned around $90° \pm 40°$, and γ rays were registered with energies up to 4 MeV. All detectors were located $\approx$14 cm from the focal point of the spectrometer. The efficiency of the array (as a function of E_γ) was calibrated through a series of source measurements, supplemented by detailed modeling [25] using the transport code MCNP [26].

A total of 103×10^6 single and higher-fold events were recorded. The data were sorted into E_γ vs TOF and $\gamma\gamma$ coincidence matrices. During the off-line sorting, the data for each detector (planar and coaxial detectors) were aligned separately in both detector pulse height and neutron time of flight, and then summed together to generate the two-dimensional (2D) matrices.

The γ-ray energy spectra shown in Fig. 1 were obtained by applying a condition on the event times corresponding to neutron energies from 1 to 8 MeV in the E_γ-TOF matrices. New γ-ray transitions found in this experiment are labeled with their energies in keV. A precise energy calibration for the planar-detector spectrum covering an energy range from 65 to 900 keV was obtained using 65 well-known in-beam γ rays as calibration points in ^{196}Pt and other isotopes. Similarly, 25 in-beam γ rays between 300 keV and 3 MeV in Pt isotopes were used for the calibration of the spectrum from the coaxial detectors. Excitation functions for the γ rays were constructed by taking 15-ns time gates [the typical full width at half maximum (FWHM) for the time resolution] in the E_γ-TOF matrices, which corresponds to a 21-keV neutron energy range at $E_n=1$ MeV. For each energy bin, a one-dimensional γ-ray pulse-height spectrum was generated and fitted with the computer code XGAM [27] over the full γ-ray energy range. An excitation function for each γ-ray transition was generated as a function of neutron energy by normalizing the γ-ray counts to the neutron flux. The neutron flux was deduced from the fission-chamber data collected simultaneously. Prompt γ rays from other ^{196}Pt$(n,xnyp\gamma)$ reactions were identified and the excitation function for each γ ray was generated up to $E_n=250$ MeV. These results and their interpretation in terms of reaction dynamics were reported separately [28].

III. LEVEL SCHEME

In this work a total of 92 transitions were observed and assigned to ^{196}Pt. These observed transitions range in γ-ray energy from 100 keV to 2.1 MeV, and all of the new transitions are above 400 keV. The absorbers used in the experiment make the observation of transitions below 100 keV energy more difficult. No new ground state transitions were observed in the excitation function measurements. Two conditions were required in order to assign transitions to levels: (i) the γ ray must be observed in the coincidence data, and (ii) the threshold energy of the γ-ray excitation function must be consistent with the placement of the level in the level scheme. The new partial level scheme is illustrated in Fig. 2. Table I summarizes all of the new levels and γ-ray transitions observed in the present work. Approximate level energies were obtained using the coincidence and the excitation-function data. The Ritz combination principle was applied to deduce exact level energies (and associated uncertainties). The relative γ-ray intensities listed in Table I include the detection efficiency. The present results confirm many of the levels and transitions observed in a previous unpublished measurement [22]. Spin assignments and limits for the levels in Table I were made by taking into account multipolarities and angular distribution calculations of Ref. [22], the neutron capture (n,γ) data from Ref. [21], and the excitation function data of the present work. The slope of excitation functions as a function of neutron energy differs for transitions from levels with different spin values. For example, a rapid rise in the cross sections as a function of incident energy is observed for low-spin transitions, while the increase in intensity is much slower for high-spin transitions. Therefore, excitation functions can be used to make approximate spin assignments. The spin assignments of the average neutron resonance (ARC) data [21] are based on the primary γ-ray transitions from the capturing states $(0^-, 1^-)$ to 0^+, 1^+, and 2^+ states. Resonances were averaged by

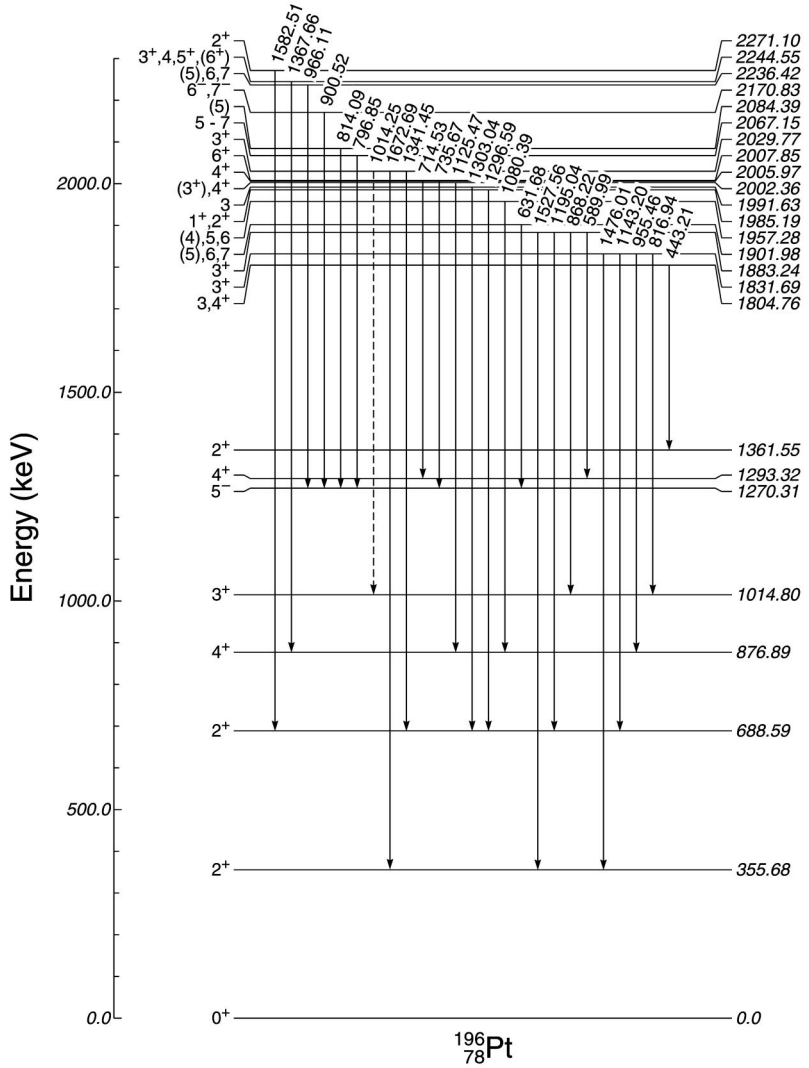

FIG. 2. Partial level scheme for ^{196}Pt, illustrating the new levels and new γ rays observed in the present work and the levels to which they decay.

employing a 2-keV neutron beam with an energy spread of 850 eV FWHM. Given the level spacing $\langle D \rangle$ in ^{196}Pt of 18 eV, the capture process is expected to average over ≈ 40 resonances. Therefore, one could state that levels with 0^+, 1^+, and 2^+ populated in the ARC data are complete below 2.5 MeV excitation. Thus, states that are not observed in the ARC data, but observed in the present data, cannot have $J = 0^+, 1^+, 2^+$ values. This statement will be referred to as ARC hereafter. Furthermore, spin assignments are made consistent with the a_2 and a_4 values in the angular distribution function $W(\theta) = 1 + a_2 P_2(\cos\theta) + a_4 P_4(\cos\theta)$ for the case $J_i \rightarrow J_f$, assuming that all mixed transitions are $E2/M1$ type (see Table II). In the following, the levels in Table I will be described in detail.

1804.76 keV; $J^\pi = (3^+)$, 4^+ level. The 443.21-keV transition to the 2^+ state restricts the spin values of this level to the 0–4 range. Due to the ARC data [21], the spin 0–2 range is eliminated. The positive a_2 and negative a_4 (at the 2σ level) values [22] favor the 443.21-keV transition to be a stretched $E2$ type. However, a $J \rightarrow J-1$ transition possibility with a mixed multipolarity cannot be completely excluded. Thus, $J^\pi = (3^+)$, 4^+ is adopted.

1831.69 keV; $J^\pi = 3^+$ level. The γ decays to the 2^+, 3^+, and 4^+ states restrict the spin values of this level to the 2–4 range. The $J = 2$ value is eliminated due to the ARC data [21]. Reference [22] reports that all of the γ rays from this level have mixed $E2/M1$ multipolarities implying the spin-parity assignment of 3^+.

1883.24 keV; $J^\pi = 3^{(+)}$ level. An $E_x = 1883(3)$ keV level was observed in a (p,p') experiment [29] and assigned $J^\pi = 4^+$. Furthermore, the 589.99-, 1195.04-, and 1527.56-keV transitions (listed in Table I) were assigned to the 4^+ 1883-keV state in Ref. [22]. However, the a_2 value of the 1527.56-keV transition was found to be $-0.36(7)$ [22], which is inconsistent with the assignment of this transition to the 4^+ level. This negative a_2 value and the ARC data [21] only permit a $J = 3$ assignment, thus suggesting a new level at 1883 keV in addition to the previously known 4^+ level at $E_x = 1883(3)$. Within the uncertainties of the a_k values, the 1527.56-keV transition can be either a mixed $E2/M1$ (implying a positive parity) or pure dipole (at the 3σ limit). One cannot rule out the possibility that the three transitions other than the 1527.56-keV γ ray may be associated with the decay of the 4^+ level. The present results suggest a closely spaced doublet at $E_x = 1883$ keV.

TABLE I. The new levels and γ rays observed with the ^{196}Pt$(n,n'\gamma)$ reaction. An 80-eV systematic uncertainty is included in the quoted γ-ray energies to take into account the deviations between the calibrated and the accepted energies [30]. A possible $\leqslant$15% angular distribution effect is not included in the relative intensities I_γ(rel). Multipolarities, a_2, and a_4 values from DiPrete *et al.* [22], are adopted wherever possible. Spin assignments and limits are derived from all available data. New levels and γ rays found in the present experiment are denoted by L and γ, respectively, in column 10.

E_i (keV)	E_γ (keV)	E_f (keV)	I_γ (rel)	Mult.	a_2	a_4	J_i^π	J_f^π	L/γ
1608.60(23)	593.80(21)	1014.80(9)	1				(5^+)	3^+	[a]
1804.76(15)	443.21(10)	1361.55(10)	1		0.24(6)	−0.17(9)	(3^+), 4^+	2^+	L, γ [b]
1831.69(14)	816.94(14)	1014.80(9)	0.719(24)	$E2/M1$	0.18(7)	−0.04(11)	3^+	3^+	L, γ [b]
	955.5(5)	876.89(9)	0.050(15)	$E2/M1$	−0.40(15)	−0.05(23)		4^+	γ [b]
	1143.2(3)	688.59(9)	0.231(20)	$E2/M1$	0.46(9)	−0.10(13)		2^+	γ [b]
	1476.01 [d]	355.68(7)	[c]	$E2/M1$	−0.11(7)	0.17(11)		2^+	γ [b]
1883.24(17)	589.99(11) [e,f]	1293.32(10)	[c]	$E2/M1$	0.36(8)	−0.00(13)	$3^{(+)}$	4^+	L, γ [b]
	868.22(19) [e]	1014.80(9)	0.680(16)					3^+	γ [b]
	1195.0(2) [e]	688.59(9)	0.320(16)	$E2/M1$	0.39(7)	0.06(10)		2^+	γ [b]
	1527.56 [d]	355.68(7)	[c]		−0.36(7)	0.18(9)		2^+	γ [b]
1901.98(15)	631.68(10)	1270.31(11)	1		0.14(23)	0.0(3)	5, 6, 7	5^-	L, γ
1957.28(22)	1080.39(20)	876.89(9)	1		0.17(5)	−0.04(8)	(4), 5^+, 6^+	4^+	L, γ
1985.2(3)	1296.6(3)	688.59(9)	1		0.04(7)	0.10(10)	1^+, 2^+	2^+	γ [b]
1991.6(4)	1303.0(4)	688.59(9)	1		−0.13(13)	0.10(19)	3, 4^+	2^+	L, γ [b]
2002.4(3)	1125.5(2)	876.89(9)	1	$E2/M1$	0.45(10)	0.06(15)	(3^+), 4^+	4^+	L, γ [b]
2005.97(14)	735.67(9)	1270.31(11)	1		0.29(7)	−0.02(9)	(4^+)	5^-	γ
2007.85(14)	714.53(10)	1293.32(10)	1				6^+	4^+	[a]
2029.8(3)	1341.4(3)	688.59(9)	0.45(4)	$E2/M1$	0.42(10)	0.13(16)	3^+	2^+	L, γ [b]
	1672.7(7)	355.68(7)	0.55(4)	$E2/M1$	−0.41(9)	−0.03(12)		2^+	γ [b]
	(1014.25) [g]	1014.80(9)						3^+	γ [b]
2067.15(15)	796.85(11)	1270.31(11)	1		−0.36(8)	−0.22(12)	5^-, 6	5^-	L, γ
2084.39(15)	814.09(11)	1270.31(11)	1		0.31(5)	−0.06(8)	4^-, 5, 6^-	5^-	L, γ
2170.83(22)	900.52(19)	1270.31(11)	1		0.21(11)	−0.14(16)	(5), $6^{(-)}$	5^-	L, γ
2236.42(24)	966.11(21)	1270.31(11)	1		0.45(5)	0.14(8)	(5), 6^-, 7^-	5^-	L, γ
2244.6(3)	1367.7(2)	876.89(9)	1		0.4(1)	0.05(15)	3^+, 4, 5^+	4^+	L, γ [b]
2271.1(4)	1582.5(4)	688.59(9)	1	$E2/M1$	0.21(14)	0.60(24)	2^+	2^+	γ [b]
$\leqslant$2500 [h]	407.06(6)								γ
$\leqslant$3000 [h]	458.31(9)								γ
$\leqslant$2500 [h]	1450.0(4)								γ

[a]Earlier values of E_i and E_γ [30] are revised in the present work.
[b]Also observed by DiPrete [22].
[c]Branching ratios could not be determined due to unresolved multiplets.
[d]As a result of unresolved multiplets, the γ-ray energies are obtained from the difference of the initial and the final level energies.
[e]γ ray that may also be associated with the known 4^+ 1883(3)-keV level [30] (see text for details).
[f]Uncertainty in the γ-ray energy was obtained by fitting the peak separately; i.e., the Ritz combination method was not used.
[g]γ ray placed tentatively based on the coincidence analysis alone.
[h]Unplaced γ ray; the approximate threshold energy from the excitation function is listed.

TABLE II. Angular distribution a_k values ($k=2$, 4) for γ-ray transitions $J_i \rightarrow J_f$ for different multipolarities (λ).

λ	a_2	a_4	$J_i \rightarrow J_f$
1	>0	0	$J \rightarrow J$
1	<0	0	$\Delta J=1$
2	<0	<0	$J \rightarrow J$
2	>0	<0	$\Delta J=2$

1901.98 keV; $J^\pi=5$, 6, 7 level. The new 631.68-keV γ ray has been used to establish this new level at 1901.98 keV. This raises a question as to whether this level is the known 1901.7-keV level [30] depopulated by the 528.1-keV transition. The excitation functions for the 631.68- and 528.1-keV γ rays are shown in Fig. 3. It is readily seen that the threshold and shape of these excitation functions do not follow similar behavior, as would be expected for transitions decaying from the same level. Given that the known 1901.7-keV level has a (8^-) spin assignment, the threshold energy in the

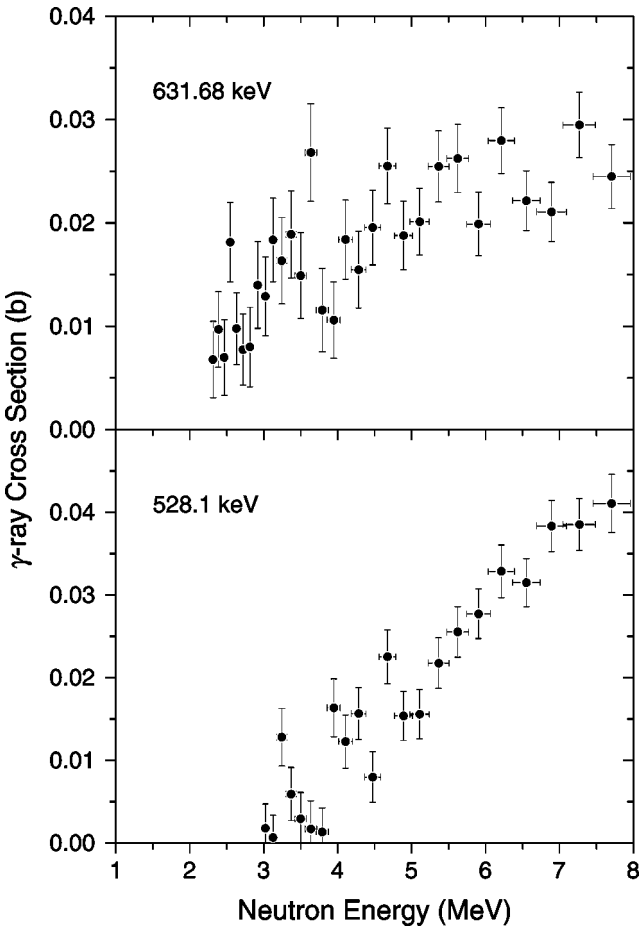

FIG. 3. Excitation functions for the 631.68- and 528.1-keV γ rays. See text for details.

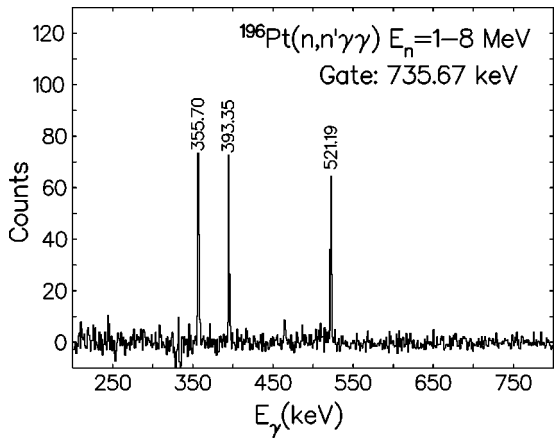

FIG. 4. Background-subtracted coincidence spectrum in the planar detectors gated on the 735.67-keV transition.

excitation function of the 528.1-keV transition is shifted to a higher neutron energy. Figure 3 shows conclusively that the 631.68-keV γ ray does not depopulate the known 1901.7-keV level. A 631-keV transition was observed in Ref. [22], but not assigned to any level.

1957.28 keV; $J^\pi=(4)$, 5^+, 6^+ level. The excitation function data of the present experiment favor a high-spin assignment. Thus, a (4), 5^+, 6^+ assignment is made. A 1080-keV γ ray was observed in Ref. [22], but not assigned to any level.

1985.19 keV; $J^\pi=1^+$, 2^+ level. This level is the known 1984.93-keV level [30]. The 1296.59-keV γ ray, observed by Cizewski *et al.* [21] but not placed, is assigned to this level both in Ref. [22] and in the present work.

1991.63 keV; $J^\pi=3$, 4^+ *level*. The decay to a 2^+ state and the ARC data [21] restrict the spins to 3, 4. As a result of the large uncertainties in the a_k values for the 1303-keV transition [22], both $J^\pi=3$ and $J^\pi=4^+$ are adopted.

2002.36 keV; $J^\pi=(3^+)$, 4^+ *level*. Using the decay to a 4^+ state and the ARC data [21], the spin values are restricted to 3–6. Since DiPrete [22] observed another transition to a 2^+ state (below the sensitivity limit in the present work), the spin can only be 3 or 4. The angular distribution measurements in Ref. [22] favor $J=4^+$.

2005.97 keV; $J^\pi=(4^+)$ *level*. This is a previously known 4^+ level without any decaying transition [30]. Figure 4 shows the coincidence spectrum observed for the 735.67-keV transition, assigned to this level. However, the positive a_2 value of this transition is inconsistent with the known spin assignment [30]. It is speculated that this transition might be contaminated. A 735-keV γ ray was observed in Ref. [22], but assigned to a new 2029-keV level.

2029.8 keV; $J^\pi=3^+$ *level*. The transitions to 2^+ states narrow the spin assignment to 0–4. The ARC data [21] eliminate spins 0–2. The $J=4$ value is eliminated based on the negative a_2 value of the 1672.69-keV γ ray, feeding the 2_1^+ level, which implies a dipole transition. If the parity were negative (i.e., $J^\pi=3^-$), the a_2 coefficient for the 1341.4-keV transition should have been negative, contrary to the experimental results.

2067.15 keV; $J^\pi=5^-$, *6 level*. Spin assignments of 5–7 were made based on the shape of the excitation function of the 796.85-keV γ ray from this level. As a result of the negative a_2 value of this transition, spin 7 is eliminated. A 796.8-keV transition was observed in Ref. [22], but not assigned to any level.

2084.39 keV; $J^\pi=4^-$, 5, 6^- *level*. The 814.09-keV γ ray was observed by DiPrete [22], but not placed in the decay scheme. From the shape of the excitation function of this transition, the spin is restricted to 4, 5, 6. The a_k coefficients for the 814.09-keV γ ray [22] that feeds the 5_1^- level suggest spin 4^-, 6^- (mixed $M1/E2$), or 5 ($J\rightarrow J$ dipole transition) assignment.

2170.83 keV; $J^\pi=(5)$, $6^{(-)}$ *level*. This new level was established based on the coincidence between the 900.52-keV, and the 393.35-, 521.19-, and 355.70-keV γ rays, ruling out the previous placement of the 900.52-keV γ ray to the $E_x=2262.3$-keV level by DiPrete [22]. The positive a_2 value (at the 2σ level) of the 900.52-keV transition that feeds the 5_1^- level rules out $E1$ type (assuming an $E2/M1$ mixing); thus the parity does not change. The decay to a 5^- level implies $J=3-7$. The shape of the excitation function favors $J=5$, 6 for this level, and we suggest $J^\pi=(5)$, $6^{(-)}$.

2236.42 keV; $J^\pi=(5)$, 6^-, 7^- *level*. The excitation function of the 966.11-keV γ ray favors spin assignments of 6 and 7 to this level; however, a spin 5 value could not be ruled

out. The 966-keV transition was previously assigned to a new 2327.8-keV level [22].

2244.6 keV; $J^\pi=3^+, 4, 5^+$ level. This level was observed as a doublet in Ref. [22], one of which was the already known 2245.56-keV 1^+, 2^+ level [30]. Based on the transition to the 4^+ state, and the ARC data [21], spin assignments are restricted to the 3–6 range. The excitation function data favor lower spins for this level; therefore, spin 6 is eliminated. The positive a_2 value of the 1367.66-keV transition feeding the 4_1^+ level permits only positive parities for spins 3 and 5.

2271.1 keV; $J^\pi=2^+$ level. This level was first observed by Cizewski [21] without any transition assigned, and was given spin values of 0^+, 1^+, 2^+. DiPrete [22] observed another transition to a 4^+ state. The angular distribution data of Ref. [22] establish $J^\pi=2^+$ to this state.

IV. IBM CALCULATIONS

^{196}Pt is a well-known example [6] of the realization of the SO(6) dynamical symmetry of the IBM. The standard formulation of the IBM describes collective excitations in nuclei in terms of bosons which carry angular momentum 0 (s boson) and 2 (d boson). The bosons can be considered as pairs of valence nucleons; e.g., ^{196}Pt, with four valence protons and eight valence neutrons, has six bosons. The model assumes one- and two-body boson interactions. If no distinction is made between proton and neutron bosons (IBM-1), the most general Hamiltonian can be expressed in terms of generators of the U(6) algebra. A dynamical symmetry occurs when the generators come from a chain of subalgebras.

In the SO(6) dynamical symmetry [5], one obtains a three-parameter analytical expression for the Hamiltonian eigenvalues, provided that the basis is classified by the subalgebra chain. In particular, one has

$$E^{\mathrm{SO}(6)}(\sigma,\tau,L)=A\sigma(\sigma+4)+B\tau(\tau+3)+CL(L+1), \tag{1}$$

where σ, τ, and L are the quantum numbers characterizing the irreducible representations of SO(6), SO(5), and SO(3), respectively. In Ref. [21], this formula was successfully fitted to the low-lying states of ^{196}Pt. The optimal choice of parameters was determined to be $A=-46.25$ keV, $B=43$ keV, and $C=23$ keV. The SO(6) dynamical symmetry describes not only the energy spectrum of the low-lying states, but also the branching ratios of the $E2$ transitions between those states.

A dynamical symmetry is usually not realized exactly and it is worth exploring how the description of ^{196}Pt can be improved when one allows for breaking of the dynamical symmetry. In particular, calculations were performed using the more general version of the model, IBM-2, that distinguishes the proton and neutron bosons. The standard IBM-2 Hamiltonian was used:

$$H=\varepsilon_\pi n_{d\pi}+\varepsilon_\nu n_{d\nu}+\kappa_{\pi\nu}Q_\pi\cdot Q_\nu+V_{\pi\pi}+V_{\nu\nu}+M_{\pi\nu}, \tag{2}$$

with

$$V_{\rho\rho}=\frac{1}{2}\kappa_\rho Q_\rho\cdot Q_\rho+\sum_{L=0,2,4}\frac{1}{2}c_{L\rho}(d_\rho^\dagger d_\rho^\dagger)^{(L)}\cdot(\tilde{d}_\rho\tilde{d}_\rho)^{(L)}, \tag{3}$$

and $Q_\rho=(d_\rho^\dagger s_\rho+s_\rho^\dagger\tilde{d}_\rho)^{(2)}+\chi_\rho(d_\rho^\dagger\tilde{d}_\rho)^{(2)}$, where $s,s^\dagger,d,d^\dagger$ are creation and destruction operators for s and d bosons, respectively, and $\rho\equiv\pi,\nu$. Here $M_{\pi\nu}$ is the Majorana interaction defined by $M_{\pi\nu}=\xi_2(s_\nu^\dagger d_\pi^\dagger-s_\pi^\dagger d_\nu^\dagger)^{(2)}\cdot(s_\nu\tilde{d}_\pi-s_\pi\tilde{d}_\nu)^{(2)}-2\Sigma_{\kappa=1,3}\xi_\kappa(d_\nu^\dagger d_\pi^\dagger)^{(\kappa)}\cdot(\tilde{d}_\nu\tilde{d}_\pi)^{(\kappa)}$, where ξ_κ are Majorana strength parameters.

Following Ref. [31], the Hamiltonian parameters were determined by using an energy-weighted least-squares fit to the excitation energies of the lowest levels. Only six parameters, however, were varied in the fit: namely, $\varepsilon=(N_\pi/N)\varepsilon_\pi+(N_\nu/N)\varepsilon_\nu$, $\chi=(N_\pi/N)\chi_\pi+(N_\nu/N)\chi_\nu$, $\kappa=\kappa_{\pi\nu}=\kappa_\rho$, $c_L=[N_\pi(N_\pi-1)c_{L\pi}+N_\nu(N_\nu-1)c_{L\nu}]/[N(N-1)]$, $L=0$, 2, 4, while the differences $\Delta\varepsilon=\varepsilon_\pi-\varepsilon_\nu=0$, $\Delta\chi=\chi_\pi-\chi_\nu=0$, $\Delta c_L=c_{L\pi}-c_{L\nu}=0$ were kept constant throughout the fit and the Majorana interaction parameters were restricted by the condition $\xi_1=\xi_2=\xi_3$ and set to 0.15 MeV which yielded the lowest 1^+ state above 2 MeV.

An important aspect of the fitting procedure was that the SO(6) dynamical symmetry was used as our starting parameters. As argued above, such parameters provide a very good description of the low-lying-level excitation energies. Thus, we might expect that the fitting procedure will not depart far from these starting parameters and we will obtain eventually only a perturbation of the SO(6) Hamiltonian. This turned out to be the case. It is straightforward to check that using $\varepsilon=0.125$ MeV, $\kappa=-0.0925$ MeV, $\chi=0$, $c_{0\pi}=c_{0\nu}=-0.53571$ MeV, $c_{2\pi}=c_{2\nu}=-0.30964$ MeV, $c_{4\pi}=c_{4\nu}=0.38036$ MeV, and a large ξ_i produces the SO(6) dynamical symmetry results corresponding to the choice of the A,B,C parameters from Ref. [21]. To determine the fit parameters, the experimental excitation energies of the lowest four 0^+ states, the lowest five 2^+ states, the lowest 3^+ state, the lowest four 4^+ states, and the lowest 5^+ and 6^+ states were used. The resulting parameters were $\varepsilon=0.553$ MeV, $\kappa=-0.1145$ MeV, $\chi=-0.036$, $c_{0\pi}=c_{0\nu}=-0.521$ MeV, $c_{2\pi}=c_{2\nu}=-0.622$ MeV, and $c_{4\pi}=c_{4\nu}=-0.3235$ MeV. The experimental results are compared with the present IBM-2 fit and the S(O6) symmetry predictions in Fig. 5. Overall the IBM-2 fit improves the agreement with experimental excitation energies. At the same time the differences between the IBM-2 fit and the SO(6) symmetry are not large, and even more importantly, the same is true for the $B(E2)$ transitions (Table III).

In the present experimental results, a new level was observed at 1804.76 keV with $J^\pi=(3^+), 4^+$. A single strong gamma transition $E_\gamma=443.21$ keV was found from this level to the 2_3^+, 1361.55 keV level. The IBM calculations predict the state 4_4^+ with SO(6) quantum numbers $\sigma=6$, $\tau=5$ around 2 MeV excitation energy, with decay to the 2_3^+, $\sigma=6$, $\tau=4$ state. In Table III, the relevant $B(E2)$ properties are shown in more detail. We note that there is another experimental 4^+ state in this energy region, at 1883 keV [29]. This state was observed in the (p,p') reaction with $L=4$

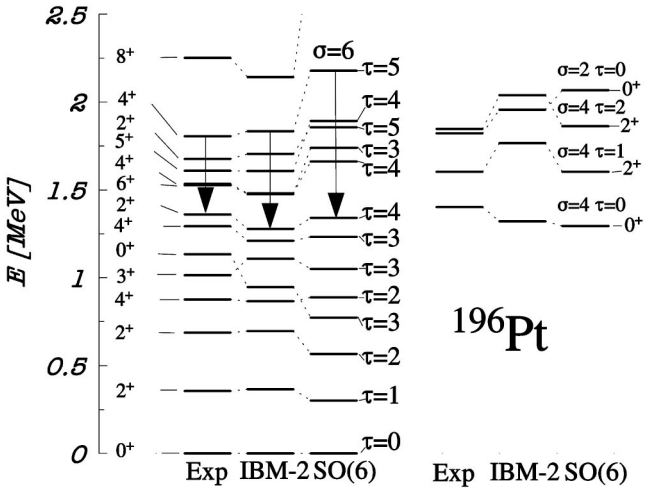

FIG. 5. Experimental and calculated excitation spectrum of ^{196}Pt. The arrows show strong transitions from the new observed level 1804.76 keV. Here σ and τ are the SO(6) quantum numbers associated with the levels.

with a substantial $B(E4)$ value. Most likely, this is a hexadecupole (or g-boson) state outside of the s,d-IBM model space. The tentative $J=(3^+)$ assignment of the new 1804.76-keV level contradicts the IBM $B(E2)$ calculation (see Table III). The proposed $\tau=5,4^+$ SO(6) assignment is consistent with a 4^+ spin-parity assignment for the 1804-keV level.

A new 3^+ level at 1831.69 keV and a proposed 3^+ state at 1883.24 keV were observed in the present experiment. In the IBM-2 calculations, 3_2^+ and the 3_3^+ states are predicted at 2065 keV and 2333 keV, respectively. The first one can be associated with the SO(6) $\sigma=6$, $\tau=6$ state, while the other is more influenced by the F-spin mixing and, therefore, an SO(6) assignment is not appropriate. The predicted decay of these states is presented in Table III. A candidate for the $\sigma=6$, $\tau=6,3^+$ state would decay predominantly to the $\sigma=6$, $\tau=5,2^+$ state at 1677 keV, with a transition too low in energy to be observed in the present work for initial states at ~ 1.8 MeV.

The 3^+ state at 1831 keV could be a candidate for the $\sigma=6$, $\tau=6,3^+$ state, because it is observed to decay to the 3^+ state at 1015 keV, albeit with a mixed $E2/M1$ transition, which would only be one degree of $\Delta\tau$ forbidden. The assignment of collective character within IBM-2 for the 1883-keV level is premature, given the uncertainty in the placement of transitions to the possible doublet of levels at this energy. Of course, levels above 1.8 MeV in excitation are also candidates for two-quasiparticle states, which would be outside of the collective IBM-2 model. Further discussions of possible IBM-2 or SO(6) assignments to the experimental levels in ^{196}Pt have to wait until additional experimental information, in particular $E2/M1$ mixing ratios, has been measured.

V. CONCLUSION

The ^{196}Pt isotope has been investigated using the $(n,n'\gamma)$ reaction with spallation neutrons from the WNR white neutron source. A total of 13 new nonyrast levels below 3 MeV were observed in this well-studied nucleus. Excitation functions and coincidence analysis of the measured γ rays and their intensities were used to expand the partial level scheme of ^{196}Pt. Spin assignments were made using all available data. IBM calculations with broken SO(6) dynamical symmetry were performed. A new experimental level was found to be a prime candidate for the $J^\pi=4^+$, $\sigma=6$, $\tau=5$ IBM state.

TABLE III. Experimental and calculated $BE(2)$ transitions in e^2b^2. The effective charges were adjusted to reproduce experimental $B(E2;2_1\rightarrow 0_1)$ in the IBM-2 calculation. The same $E2$ boson charges $e_{B\pi}=e_{B\nu}=0.154$ eb for both the IBM-2 and the SO(6) calculation, and the same χ's as in the Hamiltonians were used.

^{196}Pt	Expt. [30]	IBM-2	SO(6)
$B(E2;2_1^+\rightarrow 0_1^+)$	0.274(1)	$\equiv 0.274$	0.286
$B(E2;2_2^+\rightarrow 2_1^+)$	0.368(9)	0.348	0.374
$B(E2;2_2^+\rightarrow 0_1^+)$	0.0001	0.0007	0
$B(E2;4_1^+\rightarrow 2_1^+)$	0.405(6)	0.361	0.374
$B(E2;6_1^+\rightarrow 4_1^+)$	0.494(60)	0.366	0.381
$B(E2;0_2^+\rightarrow 2_2^+)$	0.122(68)	0.351	0.381
$B(E2;0_2^+\rightarrow 2_1^+)$	0.019(10)	0.0018	0
$B(E2;4_2^+\rightarrow 4_1^+)$	0.115(41)	0.165	0.181
$B(E2;4_2^+\rightarrow 2_2^+)$	0.196(61)	0.190	0.200
$B(E2;6_2^+\rightarrow 4_2^+)$	0.331(88)	0.214	0.230
$B(E2;4_2^+\rightarrow 2_1^+)$	0.004(1)	0.0002	0
$B(E2;6_2^+\rightarrow 4_1^+)$	0.0032(9)	0.0004	0
$B(E2;2_3^+\rightarrow 0_2^+)$	0.034(34)	0.108	0.124
$B(E2;2_3^+\rightarrow 4_1^+)$	0.0009(8)	0.0002	0
$B(E2;2_3^+\rightarrow 2_2^+)$	0.0018(16)	0.0000	0
$B(E2;2_3^+\rightarrow 0_1^+)$	0.000 02(2)	0.000 01	0
$B(E2;0_3^+\rightarrow 2_2^+)$	<0.0028	0.0016	0
$B(E2;0_3^+\rightarrow 2_1^+)$	<0.034	0.022	0
$B(E2;4_4^+\rightarrow 2_3^+)$	[a]	0.112	0.130
$B(E2;4_4^+\rightarrow 4_3^+)$	[a]	0.0185	0.0209
$B(E2;4_4^+\rightarrow 2_1^+)$	[a]	0.000 01	0
$B(E2;4_4^+\rightarrow 2_2^+)$	[a]	0.000 02	0
$B(E2;4_4^+\rightarrow 3_1^+)$	[a]	0.000 02	0
$B(E2;4_4^+\rightarrow 4_1^+)$	[a]	0.000 03	0
$B(E2;4_4^+\rightarrow 4_2^+)$	[a]	0.000 02	0
$B(E2;3_2^+\rightarrow 2_5^+)$	[a]	0.0689	0.0765 [b]
$B(E2;3_2^+\rightarrow 3_1^+)$	[a]	0.000 00	0
$B(E2;3_2^+\rightarrow 2_3^+)$	[a]	0.000 02	0
$B(E2;3_2^+\rightarrow 4_2^+)$	[a]	0.000 01	0

[a] Absolute $B(E2)$ values are not measured experimentally; calculated $B(E2)$ values are quoted for reference.

[b] $B(E2;3_3^+\rightarrow 2_5^+)$ in SO(6).

ACKNOWLEDGMENTS

The authors would like to thank Professor Steve Yates from the University of Kentucky for reading this manuscript and for providing us with D. P. DiPrete's unpublished thesis results on the spectroscopy of ^{196}Pt. This work was per-

formed under Grant No. DE-FG02-97-ER41042 (NCSU) and the grant from the National Science Foundation (RU), and was performed in part under the auspices of the U.S. Department of Energy by the University of California, Lawrence Livermore National Laboratory under Contract No. W-7405-ENG-48, and Los Alamos National Laboratory under Contract No. W-7405-ENG-36. This work has benefited from the use of the Los Alamos Neutron Science Center at Los Alamos National Laboratory. This facility is funded by the U.S. Department of Energy under Contract No. W-7405-ENG-36.

[1] C. Baktash, J.X. Saladin, J.J. O'Brien, and J.G. Alessi, Phys. Rev. C **22**, 2383 (1980).
[2] G.J. Gyapong, R.H. Spear, M.T. Esat, M.P. Fewell, A.M. Baxter, and S.M. Burnett, Nucl. Phys. **A458**, 165 (1986).
[3] F. Iachello and A. Arima, Phys. Lett. **53B**, 309 (1974).
[4] A. Arima and F. Iachello, Ann. Phys. (N.Y.) **99**, 253 (1976).
[5] A. Arima and F. Iachello, Ann. Phys. (N.Y.) **123**, 468 (1979).
[6] J.A. Cizewski, R.F. Casten, G.J. Smith, M.L. Stelts, W.R. Kane, H.G. Börner, and W.F. Davidson, Phys. Rev. Lett. **40**, 167 (1978).
[7] R.F. Casten and J.A. Cizewski, Phys. Lett. B **185**, 293 (1987), and references therein.
[8] J.K. Jewell, P.D. Cottle, K.W. Kemper, and L.A. Riley, Phys. Rev. C **56**, 2440 (1997).
[9] D.P. DiPrete, T. Belgya, E.M. Baum, E.L. Johnson, S.W. Yates, P.D. Cottle, M.A. Kennedy, and K.A. Stuckey, Phys. Rev. C **48**, 2603 (1993).
[10] N.V. Zamfir, P.D. Cottle, J.L. Johnson, and R.F. Casten, Phys. Rev. C **48**, 1745 (1993).
[11] P. von Brentano *et al.*, Phys. Rev. Lett. **76**, 2029 (1996).
[12] N. Pietralla, P. von Brentano, R.-D. Herzberg, U. Kneissl, J. Margraf, H. Maser, H.H. Pitz, and A. Zilges, Phys. Rev. C **52**, R2317 (1995).
[13] C. Rangacharyulu, A. Richter, H.J. Wortche, W. Ziegler, and R.F. Casten, Phys. Rev. C **43**, R949 (1991).
[14] N. Lo Iudice and A. Richter, Phys. Lett. B **304**, 193 (1993).
[15] C. Baktash, J.X. Saladin, J.J. O'Brien, and J.G. Alessi, Phys. Rev. C **18**, 131 (1978).
[16] C.Y. Chen, J.X. Saladin, and A.A. Hussein, Phys. Rev. C **28**, 1570 (1983).
[17] A. Mauthofer, K. Stelzer, J. Idzko, Th.W. Elze, H.J. Wollersheim, H. Emling, P. Fuchs, E. Grosse, and D. Schwalm, Z. Phys. A **336**, 263 (1990).
[18] I.Y. Lee, D. Cline, P.A. Butler, R.M. Diamond, J.O. Newton, R.S. Simon, and F.S. Stephens, Phys. Rev. Lett. **39**, 684 (1977).
[19] J.A. Cizewski, E.R. Flynn, R.E. Brown, and J.W. Sunier, Phys. Lett. **88B**, 207 (1979).
[20] P.T. Deason, C.H. King, T.L. Khoo, J.A. Nolen, Jr., and F.M. Bernthal, Phys. Rev. C **20**, 927 (1979).
[21] J.A. Cizewski, R.F. Casten, G.J. Smith, M.R. Macphail, M.L. Stelts, W.R. Kane, H.G. Börner, and W.F. Davidson, Nucl. Phys. **A323**, 349 (1979), and references therein.
[22] D. P. DiPrete, Ph.D. thesis, University of Kentucky, 1994 (unpublished).
[23] J.A. Becker and R.O. Nelson, Nucl. Phys. News **7**, 11 (1997).
[24] S.A. Wender, S. Balestrini, A. Brown, R.C. Haight, C.M. Laymon, T.M. Lee, P.W. Lisowski, W. McCorkle, R.O. Nelson, W. Parker, and N.W. Hill, Nucl. Instrum. Methods Phys. Res. A **336**, 226 (1993).
[25] D. P. McNabb, ''Uncertainty Budget and Efficiency Analysis for the ^{239}Pu$(n,2n\gamma)$ Partial Reaction Cross-Section Measurements,'' Technical Report No. UCRL-ID-139906, Lawrence Livermore National Laboratory, 1999.
[26] J. F. Briesmeister, ''A General Monte Carlo Code for Neutron and Photon Transport,'' Technical Report No. LA-7396-M-Rev. 2, Los Alamos National Laboratory, 1986.
[27] W. Younes (unpublished).
[28] E. Tavukcu, L.A. Bernstein, K. Hauschild, J.A. Becker, P.E. Garrett, C.A. McGrath, D.P. McNabb, W. Younes, M.B. Chadwick, R.O. Nelson, G.D. Johns, and G.E. Mitchell, Phys. Rev. C **64**, 054614 (2001).
[29] P.T. Deason, C.H. King, R.M. Ronningen, T.L. Khoo, F.M. Bernthal, and J.A. Nolen, Jr., Phys. Rev. C **23**, 1414 (1981).
[30] Z. Chunmei, W. Gongqing, and T. Zhenlan, Nucl. Data Sheets **83**, 145 (1998).
[31] P. Navrátil, B.R. Barrett, and J. Dobeš, Phys. Rev. C **53**, 2794 (1996).